PERGAMON

International Journal of Solids and Structures 37 (2000) 2625–2637

INTERNATIONAL JOURNAL OF SOLIDS and STRUCTURES

www.elsevier.com/locate/ijsolstr

Saint-Venant end effects in piezoceramic materials

Xiaoping Ruan[a], Stephen C. Danforth[b], Ahmad Safari[b], Tsu-Wei Chou[a,*]

[a]*Center for Composite Materials and Department of Mechanical Engineering, University of Delaware, Newark, DE 19716, USA*

[b]*Department of Ceramic and Material Engineering and Center for Ceramic Research, Rutgers, The State University of New Jersey, Piscataway, NJ 08855, USA*

Received 22 November 1997; received in revised form 1 July 1998

Abstract

The stress decay rate and characteristic decay length for anisotropic materials and fiber composites have been intensively investigated. However, those for piezoelectric materials have not been studied. In this paper, we examine the Saint-Venant end effects of piezoceramic materials by considering the problem of a semi-infinite piezoceramic strip polarized in the thickness direction and with applied voltages on the upper and lower surfaces. It is assumed that the gradient of electric potential in the axial direction is much smaller than that in the thickness direction. Thus, the governing equations in terms of the Airy stress function and electric potential function can be uncoupled. The governing equation in terms of the Airy stress function involves only two non-dimensional parameters after non-dimensionalization. Finally, the stress decay rates and characteristic decay lengths for a variety of piezoceramic materials are computed numerically, and their variation with the two non-dimensional parameters is presented.

Keywords: Piezoelectricity; Saint-Venant principle; Piezoceramic; Stress decay rate

1. Introduction

Saint-Venant end effects can be characterized quantitatively by the decay rate or the characteristic decay length of the physical field. It is well known that the characteristic decay length is about the width of the member under loading for homogeneous isotropic materials, and it is greater than the width for anisotropic materials. Thus, Saint-Venant end effects cannot be neglected.

Recent developments in the research on Saint-Venant's principle can be found in review articles by Horgan (1989, 1996). The exact decay rate in an anisotropic elastic strip using analogs of the Papkovich–Fadle eigenfunctions has been investigated by Choi and Horgan (1977) and the decay rates

* Corresponding author. Tel.: 001-302-831-2421; Fax: 001-302-831-3619.
E-mail address: chou@me.udel.edu (T.W. Chou).

0020-7683/00/$ - see front matter
PII: S0020-7683(99)00034-7

and the characteristic decay lengths for a variety of contemporary engineering and composite materials were given by Miller and Horgan (1995). Research works of Saint-Venant's principle can be found in the fields of non-linear elasticity, viscous flows, transient heat conduction and elastodynamics (Horgan, 1996).

Significant advances have been made in recent years in the technologies of piezoelectric materials and their applications, for example, in intelligent structures (Newnham, 1997), various types of metal–ceramic composite actuators (Newnham et al., 1992; Dogan and Newnham, 1994), and multi-phase piezoelectric composite transducers (Zhang et al., 1995). Thus, it is desirable to expand the study of Saint-Venant's principle into piezoelectric materials, and this paper is devoted to the study of the stress decay rate in piezoceramics.

The boundary value problem in the present study considers a semi-infinite piezoceramic strip polarized in the thickness direction, subject to voltages and traction-free boundary conditions on the upper and lower surfaces and self-equilibrated end loading. It is first assumed that the gradient of electric potential in the axial direction is much smaller than that in the thickness direction. Thus, the governing equations in terms of the Airy stress function and electric potential function can be uncoupled, and the governing equation in terms of the Airy stress function involves only two non-dimensional parameters. Finally, the stress decay rates and characteristic decay lengths for a variety of piezoceramic materials are computed numerically, and their variations with the two non-dimensional parameters are presented.

2. Theory

2.1. Constitutive equations and governing equations of piezoelectricity

In linear piezoelectricity, the equations of linear elasticity are coupled to the charge equation of electrostatics by means of the piezoelectric constants. The constitutive equations of piezoelectricity can be stated in the following general form (see Tiersten, 1969):

$$\{S\} = [s]\{\sigma\} + [d]\{E\} \tag{1}$$

and

$$\{D\} = [d]^T\{\sigma\} + [\epsilon]\{E\}, \tag{2}$$

where $\{\sigma\}$ is the stress tensor in contracted notation, $\{S\}$ the strain tensor in contracted notation, $\{E\}$ the electric field vector, $\{D\}$ the electric displacement vector, $[s]$ the elastic compliance matrix, $[d]$ the piezoelectric matrix and $[\epsilon]$ the dielectric permittivity matrix. The equation of motion and the charge equation of electrostatics are, respectively,

$$\sigma_{ij,i} + f_j = \rho\ddot{u}_j \tag{3}$$

and

$$D_{i,i} = 0, \tag{4}$$

where σ_{ij} are the components of the stress tensor, f_j are the components of the body force, u_j are the component of displacement, D_i are the components of the electric displacement and ρ is the density.

Consider a 2-D problem in the x_1–x_3 plane. If the x_3-axis is taken as the polarization direction, the constitutive equation for a piezoelectric ceramic can be written as follows:

$$\begin{Bmatrix} S_1 \\ S_3 \\ S_5 \end{Bmatrix} = \begin{bmatrix} s_{11} & s_{13} & 0 \\ s_{13} & s_{33} & 0 \\ 0 & 0 & s_{55} \end{bmatrix} \begin{Bmatrix} \sigma_1 \\ \sigma_3 \\ \sigma_5 \end{Bmatrix} + \begin{bmatrix} 0 & d_{31} \\ 0 & d_{33} \\ d_{15} & 0 \end{bmatrix} \begin{Bmatrix} E_1 \\ E_3 \end{Bmatrix} \tag{5}$$

and

$$\begin{Bmatrix} D_1 \\ D_3 \end{Bmatrix} = \begin{bmatrix} 0 & 0 & d_{15} \\ d_{31} & d_{33} & 0 \end{bmatrix} \begin{Bmatrix} \sigma_1 \\ \sigma_3 \\ \sigma_5 \end{Bmatrix} + \begin{bmatrix} \epsilon_{11} & 0 \\ 0 & \epsilon_{33} \end{bmatrix} \begin{Bmatrix} E_1 \\ E_3 \end{Bmatrix}. \tag{6}$$

The equation of equilibrium (with zero body force) and the compatibility equation are, respectively,

$$\frac{\partial \sigma_1}{\partial x_1} + \frac{\partial \sigma_5}{\partial x_3} = 0, \tag{7}$$

$$\frac{\partial \sigma_5}{\partial x_1} + \frac{\partial \sigma_3}{\partial x_3} = 0$$

and

$$\frac{\partial^2 S_1}{\partial x_3^2} + \frac{\partial^2 S_3}{\partial x_1^2} = \frac{\partial^2 S_5}{\partial x_1 \partial x_3}. \tag{8}$$

2.2. Governing equations in terms of Airy stress function and electric potential

Substituting the constitutive equation Eq. (5) into the compatibility equation Eq. (8), we get

$$\frac{\partial^2}{\partial x_3^2}[s_{11}\sigma_1 + s_{13}\sigma_3 + d_{31}E_3] + \frac{\partial^2}{\partial x_1^2}[s_{13}\sigma_1 + s_{33}\sigma_3 + d_{33}E_3] = \frac{\partial^2}{\partial x_1 \partial x_3}[s_{55}\sigma_5 + d_{15}E_1], \tag{9}$$

which is expressed in terms of the stress and electric fields. Substituting the constitutive equation Eq. (6) into the charge equation Eq. (4) yields

$$\frac{\partial}{\partial x_1}[d_{15}\sigma_5 + \epsilon_{11}E_1] + \frac{\partial}{\partial x_3}[d_{31}\sigma_1 + d_{33}\sigma_3 + \epsilon_{33}E_3] = 0, \tag{10}$$

which is also given in terms of the stress and electrical fields.

The Airy stress function $f(x_1,x_2)$ is defined such that

$$\sigma_1 = \frac{\partial^2 f}{\partial x_3^2},$$

$$\sigma_3 = \frac{\partial^2 f}{\partial x_1^2}$$

and

$$\sigma_5 = -\frac{\partial^2 f}{\partial x_1 \partial x_3}. \tag{11}$$

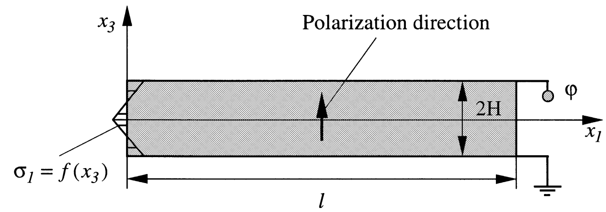

Fig. 1. A semi-infinite piezoceramic strip with electric and stress boundary conditions.

The equations of equilibrium Eq. (7) are then identically satisfied. An electric potential, φ, exists if there is no dissipation of energy and the electric field can be expressed as:

$$E_1 = -\frac{\partial\varphi}{\partial x_1}$$

and

$$E_3 = -\frac{\partial\varphi}{\partial x_3}. \tag{12}$$

Finally, substituting the Airy stress function and electric potential into Eqs. (9) and (10), we obtain the following governing equations:

$$s_{11}\frac{\partial^4 f}{\partial x_3^4} + (2s_{13} + s_{55})\frac{\partial^4 f}{\partial x_1^2 \partial x_3^2} + s_{33}\frac{\partial^4 f}{\partial x_1^4} = d_{31}\frac{\partial^3\varphi}{\partial x_3^3} + (d_{33} - d_{15})\frac{\partial^3\varphi}{\partial x_1^2 \partial x_3} \tag{13}$$

and

$$\epsilon_{11}\frac{\partial^2\varphi}{\partial x_1^2} + \epsilon_{33}\frac{\partial^2\varphi}{\partial x_3^2} = d_{31}\frac{\partial^3 f}{\partial x_3^3} + (d_{33} - d_{15})\frac{\partial^3 f}{\partial x_1^2 \partial x_3}, \tag{14}$$

which involve nine independent elastic, piezoelectric and dielectric constants.

2.3. Governing equations for a piezoelectric strip

Consider a semi-infinite piezoceramic strip that occupies the region $x_1 \geq 0$ and $-H \leq x_3 \leq H$, as shown in Fig. 1. Here, H is the half thickness of the strip. The strip is polarized in the x_3-direction. There is no mechanical loading on the upper and lower surfaces, while a prescribed self-equilibrated mechanical loading is applied on the end surface $x_1 = 0$. Constant voltages are also applied on the upper and lower surfaces of the piezoceramic strip.

For the purpose of the present study, it is reasonable to assume that the x_3 component of the electric field, E_3, is much greater than the x_1 component, E_1, i.e. $|\varphi_{,3}| \gg |\varphi_{,1}|$. If it is further assumed that $|\varphi_{,33}|$ is much greater than $|\varphi_{,11}|$, we can neglect the last term of Eq. (13) and the first term of Eq. (14). Then, Eqs. (13) and (14) yield

$$s_{11}\frac{\partial^4 f}{\partial x_3^4} + (2s_{13} + s_{55})\frac{\partial^4 f}{\partial x_1^2 \partial_3^2} + s_{33}\frac{\partial^4 f}{\partial x_1^4} = d_{31}\frac{\partial^3\varphi}{\partial x_3^3} \tag{15}$$

and

$$\epsilon_{33}\frac{\partial^2\varphi}{\partial x_3^2} = d_{31}\frac{\partial^3 f}{\partial x_3^3} + (d_{33} - d_{15})\frac{\partial^3 f}{\partial x_1^2 \partial x_3}. \tag{16}$$

Taking the partial derivative of Eq. (16) with respect to x_3 and then substituting it into Eq. (15), the governing equation in terms of the stress function only is obtained:

$$s_{33}\frac{\partial^4 f}{\partial x_1^4} + \left[(2s_{13} + s_{55}) - \frac{d_{31}}{\epsilon_{33}}(d_{33} - d_{15})\right]\frac{\partial^4 f}{\partial x_1^2 \partial x_3^2} + \left(s_{11} - \frac{d_{31}^2}{\epsilon_{33}}\right)\frac{\partial^4 f}{\partial x_3^4} = 0. \tag{17}$$

It should be noted that the above assumptions regarding the electric fields, E_1 and E_3, and the resulting governing equation Eq. (17) have been adopted by the authors in a recent study of the electromechanical responses of piezoceramic materials (Ruan et al., 1999).

2.4. Non-dimensionalization

The governing partial differential equations (Eqs. (16) and (17)) are first non-dimensionalized. The dimensionless co-ordinates, ξ and η, are defined as:

$$\xi = \left(\frac{s_{11}}{s_{33}}\right)^{1/4}\frac{x_1}{H}$$

and

$$\eta = \frac{x_3}{H}. \tag{18}$$

Also, by defining the following non-dimensional parameters

$$\beta_1 = \left(\frac{1}{s_{11}s_{33}}\right)^{1/2}(2s_{13} + s_{55}),$$

$$\beta_2 = \frac{d_{31}^2}{\epsilon_{33}s_{11}},$$

$$\beta_3 = \left(\frac{1}{s_{11}s_{33}}\right)^{1/2}\frac{d_{31}}{\epsilon_{33}}(d_{33} - d_{15}),$$

$$k_1 = \beta_1 - \beta_3,$$

$$k_2 = 1 - \beta_2 \tag{19}$$

and the dimensional constant

$$\kappa = \frac{d_{31}}{s_{11}},$$

the governing partial differential equations (Eqs. (16) and (17)) become, respectively,

$$\frac{\partial^4 f}{\partial \xi^4} + k_1 \frac{\partial^4 f}{\partial \xi^2 \partial \eta^2} + k_2 \frac{\partial^4 f}{\partial \eta^4} = 0 \tag{20}$$

and

$$\frac{\partial^2 \varphi}{\partial \eta^2} = \frac{1}{H}\frac{\beta_3}{\kappa}\frac{\partial^3 f}{\partial \xi^2 \partial \eta} + \frac{1}{H}\frac{\beta_2}{\kappa}\frac{\partial^3 f}{\partial \eta^3}. \tag{21}$$

The governing equations in the above form involve three non-dimensional parameters and one dimensional constant instead of the nine material constants. It should be noted that Eq. (20) pertains to the Airy stress function only and it does not involve the electric potential function.

3. Eigenconditions

Considering the self-equilibrium condition at each x_1 (or ξ) section of the strip, the following relations in terms of the Airy stress function are adopted for the traction-free boundary conditions.

$$f(\xi,\eta) = 0$$

and

$$\frac{\partial f(\xi,\eta)}{\partial \eta} = 0 \text{ at } \eta = \pm 1. \tag{22}$$

These are justified, since Eq. (22) implies

$$\frac{\partial^2 f(\xi,\eta)}{\partial \xi^2} = 0$$

and

$$\frac{\partial^2 f(\xi,\eta)}{\partial \xi \partial \eta} = 0 \text{ at } \eta = \pm 1. \tag{23}$$

Following the approach described by Miller and Horgan (1995), we seek solutions of Eq. (20) of the form:

$$f(\xi,\eta) = e^{-\gamma\xi} F(\eta), \tag{24}$$

where γ is a complex constant. The form of $f(\xi,\eta)$ ensures that the stresses decay exponentially in the x_1-direction. Substituting Eq. (24) into Eq. (20) yields the following fourth-order ordinary differential equation:

$$k_2 F''''(\eta) + k_1 \gamma^2 F''(\eta) + \gamma^4 F(\eta) = 0 \tag{25}$$

and boundary conditions:

$$F(\eta) = 0$$

and

$$F'(\eta) = 0 \text{ at } \eta = \pm 1. \tag{26}$$

Eqs. (25) and (26) constitute an eigenvalue problem with eigenparameter γ.

A solution of Eq. (25) is sought in the form

$$F(\eta) = Ae^{\lambda\eta},\ \lambda = \text{constant}. \tag{27}$$

Substituting the above expression into Eq. (25), the following characteristic equation is obtained:

$$k_2\lambda^4 + k_1\gamma^2\lambda^2 + \gamma^4 = 0. \tag{28}$$

The roots of Eq. (28) are

$$\lambda = \pm\frac{\gamma}{\sqrt{2k_2}}\sqrt{-k_1 \pm \sqrt{k_1^2 - 4k_2}}. \tag{29}$$

Considering the case $k_1 > 0$ and $k_2 > 0$, which is valid for all the piezoceramics studied here, the four roots of λ can be denoted as:

$$\lambda_{1,2} = (p_1 \pm iq_1)\gamma$$

and

$$\lambda_{3,4} = (p_2 \pm iq_2)\gamma, \tag{30}$$

where $i = \sqrt{-1}$, p_1 and q_1 are the real and imaginary parts of λ_1, and p_2 and q_2 are the real and imaginary parts of λ_3. We now study the following three cases separately.

Case A. ($k_1^2 - 4k_2 < 0$):

In this case, it can be shown that the roots λ can be represented as:

$$\lambda_{1,2} = (p \pm iq)\gamma$$

and

$$\lambda_{3,4} = (-p \pm iq)\gamma, \tag{31}$$

where

$$p = \frac{1}{2\sqrt{k_2}}\sqrt{2\sqrt{k_2} - k_1}$$

and

$$q = \frac{1}{2\sqrt{k_2}}\sqrt{2\sqrt{k_2} + k_1}. \tag{32}$$

Substituting Eq. (31) into Eq. (26), we obtain

$$F(\eta) = e^{\gamma p\eta}(C_1 \cos\gamma q\eta + C_2 \sin\gamma q\eta) + e^{-\gamma p\eta}(C_3 \cos\gamma q\eta + C_4 \sin\gamma q\eta), \tag{33}$$

where C_1, C_2, C_3 and C_4 are integration constants. It can be shown that if $F(\eta)$ is an even function, which corresponds to symmetric deformations, $C_3 = C_1$ and $C_4 = -C_2$. Thus, Eq. (33) becomes

$$F(\eta) = C_1 \cosh(p\gamma\eta)\cos(\gamma q\eta) + C_2 \sinh(p\gamma\eta)\sin(q\gamma\eta). \tag{34}$$

By applying the boundary conditions (26), the eigencondition (characteristic equation) is obtained as follows:

$$\frac{\sinh(2\gamma p)}{p} + \frac{\sin(2\gamma q)}{q} = 0. \tag{35}$$

Similarly, if $F(\eta)$ is an odd function, which corresponds to anti-symmetric deformations, the eigencondition can be expressed as:

$$\frac{\sinh(2\gamma p)}{p} - \frac{\sin(2\gamma q)}{q} = 0. \tag{36}$$

Thus, it is convenient to study the eigencondition by separating the eigenfunctions into even and odd functions.

Case B. ($k_1^2 - 4k_2 = 0$):

In this case, we have

$$\lambda_{1,2} = p\gamma i$$

and

$$\lambda_{3,4} = -p\gamma i, \tag{37}$$

where

$$p = \sqrt{\frac{k_1}{2k_2}}.$$

The eigenconditions for even and odd eigenfunctions are, respectively,

$$\sin(2\gamma p) + 2\gamma p = 0 \tag{38}$$

and

$$\sin(2\gamma p) - 2\gamma p = 0. \tag{39}$$

It can be readily shown that an isotropic elastic material is a limiting case of Case B, for which $p = 1$.

Case C. ($k_1^2 - 4k_2 > 0$):

In this case, we have

$$\lambda_{1,2} = \pm p\gamma i$$

and

$$\lambda_{3,4} = \pm q\gamma i, \tag{40}$$

where

$$p = \sqrt{\frac{k_1 - \sqrt{k_1^2 - 4k_2}}{2k_2}}$$

and

$$q = \sqrt{\frac{k_1 + \sqrt{k_1^2 - 4k_2}}{2k_2}}. \tag{41}$$

The eigenconditions for even and odd eigenfunctions are, respectively,

$$p\cos(q\gamma)\sin(p\gamma) - q\cos(p\gamma)\sin(q\gamma) = 0 \tag{42}$$

and

$$p\cos(p\gamma)\sin(q\gamma) - q\sin(p\gamma)\cos(q\gamma) = 0. \tag{43}$$

It should be noted that the expressions of eigenconditions (Eqs. (35), (36), (38), (39), (42) and (43)) derived above are in the same form as those obtained by Choi and Horgan (1977).

4. Stress decay rate and characteristic decay length

For the three cases discussed in Section 3, the eigenvalues can be determined from the corresponding eigenconditions. From Eq. (24), we see that the decay rate in the dimensionless coordinates is the eigenvalue with the smallest positive real part. Once the decay rate is obtained, it should be transformed back to the variable x_1 to obtain the decay rate in the original coordinates. Suppose t^* is the smallest positive real part of the eigenvalue in the dimensionless coordinates; then the stresses decay as $e^{-t^*\xi}$. By transforming back to the original coordinates, it can be seen that the stresses decay as $e^{-k^*x_1}$ in the original coordinates, where

$$k^* = \left(\frac{s_{11}}{s_{33}}\right)^{1/4}\frac{t^*}{H}. \tag{44}$$

Following Miller and Horgan (1995), the characteristic decay length λ^* is defined as the length over which the solution of the Airy stress function, and hence the stress τ, decays to 1% of its value at $x_1 = 0$

$$\left|\tau(\lambda^*, x_3)\right| = Ae^{-k^*\lambda^*} = A\frac{1}{100}. \tag{45}$$

Then we obtain

$$\lambda^* = \frac{\ln 100}{k^*}. \tag{46}$$

Now, we summarize the procedure for determining stress decay rates and characteristic decay lengths for piezoceramic materials as follows:

1. Determine the non-dimensional parameters, β_1, β_2 and β_3, and hence k_1 and k_2, using the elastic, piezoelectric and dielectric constants of piezoceramic materials;
2. Determine the characteristic equations based upon the magnitude of $k_1^2 - 4k_2$;
3. Find the complex roots of characteristic equations using Muller's method, whose FORTRAN subroutine is available in computer mathematics library (Visual Numerics, 1994);

Table 1
Elastic, piezoelectric and dielectric constants of some selected piezoceramics

	PZT-5H[1]	PZT-5[2]	PZT-4[3]	Ceramic-B[1]	VIBRIT 200[4]	VIBRIT 525[4]
Elastic compliance (10^{-12} m^2/N)						
s_{11}	16.5	16.4	12.4	8.6	11.1	15.7
s_{12}	−4.78	−5.74	−3.98	−2.6	−4.4	−5.9
s_{13}	−8.45	−7.22	−5.52	−2.7		
s_{33}	20.7	18.8	16.1	9.1	12.1	19.3
s_{44}	43.5	47.5	39.1	22.2	27.0	46.0
Piezoelectric constant (10^{-12} C/N)						
d_{31}	−274	−172	−135	−58	−80	−190
d_{33}	593	374	300	149	170	420
d_{15}	741	584	525	242	220	625
Relative permittivity ($\epsilon_0 = 8.85 \times 10^{-12}$ F/m)						
ϵ_{11}/ϵ_0	1700	1730	1470	1000	900	2000
ϵ_{33}/ϵ_0	1470	1700	1300	910	1030	2000

[1] Data Sheet (1990).
[2] Rogacheva (1994).
[3] Park and Sun (1995).
[4] Zelenka (1986).

4. Determine the smallest positive real parts of the eigenvalues; and
5. Determine the decay rates and characteristic decay length using Eqs. (44) and (46).

5. Results

In order to justify the assumption of $|\varphi_{,3}| \gg |\varphi_{,1}|$ made in this paper, a numerical example is performed to examine its suitability. Consider the piezoelectric strip shown in Fig. 1; the geometric parameters are $l = 10$ mm and $H = 1$ mm. The electric potentials are $\varphi = 100$ V on the upper edge and $\varphi = 0$ on the lower edge. The mechanical loading on the end surface $x_1 = 0$ is (units = N/mm^2)

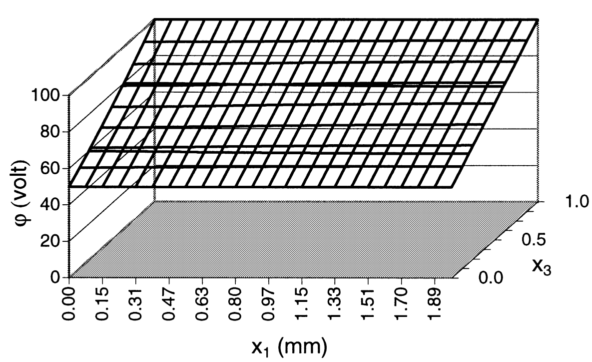

Fig. 2. Distribution of the electric potential in the one-half piezoceramic strip using FEM approach.

Table 2
Decay rate and characteristic decay length for some selected piezoceramics

	Non-dimensional parameter		Decay rate k^*	Characteristic decay length λ^*	Decay length with zero electric field
	k_1	k_2			
PZT-5H	1.27	0.65	$1.71/H$	$1.35 \times 2H$	$1.22 \times 2H$
PZT-5	1.74	0.88	$1.93/H$	$1.19 \times 2H$	$1.15 \times 2H$
PZT-4	1.80	0.87	$1.89/H$	$1.22 \times 2H$	$1.17 \times 2H$
Ceramic-B	1.82	0.95	$2.03/H$	$1.13 \times 2H$	$1.12 \times 2H$
VIBRIT 200	1.53	0.94	$1.94/H$	$1.19 \times 2H$	$1.17 \times 2H$
VIBRIT 525	1.84	0.87	$1.92/H$	$1.20 \times 2H$	$1.16 \times 2H$
Isotropic	2.0	1.0	$2.11/H$	$1.09 \times 2H$	

$$\sigma_1 = 2x_3 - 1,\; x_3 \geq 0$$

and

$$\sigma_1 = -2x_3 - 1,\; x_3 < 0. \tag{47}$$

PZT-5H, whose material properties are shown in Table 1, is used. The commercially available FEM code, ABAQUS, is adopted. We use 320 8-nodal serendipity elements for one-half of the piezoceramic strip. The distribution of the electric potential in one-half of the piezoceramic strip is shown in Fig. 2. It can be seen that the variation of the electric potential, φ, is almost linear along the x_3 axis, and there is a very small variation of φ along the x_1 axis.

Table 1 lists the data of the elastic, piezoelectric and dielectric constants of some selected piezoceramic materials. The elastic compliance constant s_{ij} and piezoelectric strain constant d_{ij} of PZT-4 given in Table 1 have been transformed, respectively, from the elastic stiffness c_{ij}, and piezoelectric stress coefficient e_{ij}. Since s_{13} of VIBRIT 200 and 525 are not available in the original reference, it is assumed that $s_{13}=s_{12}$ in order to determine the parameter β_1, and hence k_1. In Table 2, the values of non-dimensional parameters, k_1 and k_2, and the decay rates and lengths corresponding to the six selected piezoceramics are presented. In Table 3, the variation of non-dimensional characteristic decay lengths with non-dimensional parameters, k_1 and k_2, is presented.

The results of Tables 2 and 3 are obtained by using Eqs. (35), (38) and (42), which respond to

Table 3
Variation of non-dimensional characteristic decay lengths, $\lambda^*/2H$, with non-dimensional parameters, k_1 and k_2

$k_1\backslash k_2$	0.1	0.2	0.3	0.4	0.5	0.6	0.7	0.8	0.9	1.0
0.2	2.3897	2.0554	1.8765	1.7572	1.6690	1.5997	1.5430	1.4954	1.4544	1.4186
0.4	2.2237	1.9487	1.7948	1.6898	1.6110	1.5485	1.4970	1.4534	1.4157	1.3827
0.6	2.0796	1.8544	1.7214	1.6286	1.5580	1.5014	1.4544	1.4144	1.3797	1.3491
0.8	1.9443	1.7686	1.6544	1.5724	1.5090	1.4577	1.4147	1.3780	1.3459	1.3175
1.0	1.7774	1.6878	1.5920	1.5200	1.4633	1.4168	1.3775	1.3437	1.3140	1.2877
1.2	2.2712	1.6063	1.5324	1.4705	1.4201	1.3781	1.3423	1.3112	1.2838	1.2593
1.4	2.6187	1.5048	1.4730	1.4227	1.3788	1.3413	1.3088	1.2803	1.2550	1.2323
1.6	2.8868	1.7684	1.4077	1.3748	1.3385	1.3057	1.2765	1.2506	1.2274	1.2064
1.8	3.1175	2.0291	1.2987	1.3236	1.2979	1.2706	1.2451	1.2218	1.2007	1.1814
2.0	3.3250	2.2196	1.6458	1.2568	1.2546	1.2350	1.2138	1.1935	1.1745	1.1549

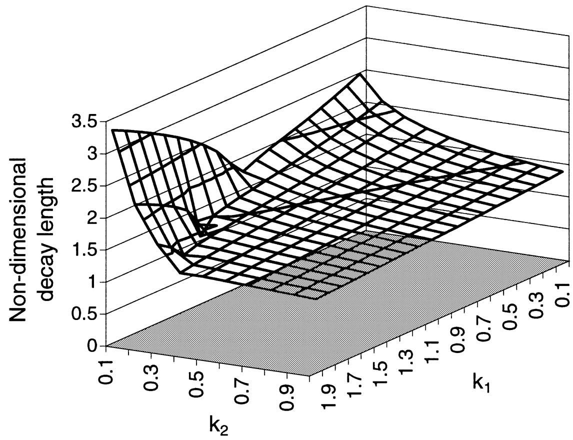

Fig. 3. Graph of non-dimensional characteristic decay length, $\lambda^*/2H$, vs. non-dimensional parameters, k_1 and k_2.

symmetric end loading. It can be seen that for $d_{31}=0$ and $d_{33}-d_{15}=0$, the terms on the right-hand side of Eq. (13) vanish and, consequently, $\beta_2=0$, $\beta_3=0$, $k_1=\beta_1$, and $k_2=1$. This corresponds to the case of an orthotropic elastic medium. The decay rates and decay lengths for isotropic materials as well as these piezoceramic materials with uniform electric potential are also presented in Table 2. The ranges of k_1 and k_2 of these piezoceramics are 1.27–1.84 and 0.65–0.95, respectively. The ranges of stress decay rates and decay lengths are $1.71/H$–$2.03/H$ and $1.13\times 2H$–$1.35\times 2H$, respectively.

The characteristic decay lengths of the piezoceramics discussed in this paper are larger than those of isotropic materials, and the decay lengths of these piezoceramic materials with electric fields are larger than those of the same materials with zero electric field. The stress decay length, for instance, of PZT-5H with an applied electric field is about 24% longer than that for isotropic materials and about 11% longer than that of the same material with zero electric field.

The ranges of $k_1=0.1$–2.0 and $k_2=0.1$–1.0 are chosen for parametric studies. It can be seen from Table 3 and Fig. 3 that the stress decay lengths decrease with increase of parameter k_1 for a given value of parameter k_2. At $k_1=2.0$ and $k_2=1.0$, which corresponds to isotropic materials, the decay length reaches its minimum, and at $k_1=2.0$ and $k_2=0.1$, the maximum decay length occurs.

6. Conclusions and discussion

1. Since the voltage is added to the upper and lower edges of the strip, the assumption of $|\varphi_{,3}|\gg|\varphi_{,1}|$ implies that the x_1-direction electric field $|\varphi_{,1}|$, induced by the stress field, is much smaller than that induced by the applied voltage. The numerical results from the FEM approach justify this assumption.
2. Based upon the assumption that $|\varphi_{,3}|\gg|\varphi_{,1}|$, the governing equations in terms of the Airy stress function and electric potential function are uncoupled, and only two non-dimensional parameters appear in the dimensionless equation.
3. It can be seen from Eq. (19) that β_1 consists of elastic compliance constants only, and β_2 and β_3 are expressed in terms of the elastic, piezoelectric and dielectric constants. Therefore, the parameters β_2 and β_3 represent the piezoelectric effect on the stress field. For instance, if $\beta_2=0$ and $\beta_3=0$, and hence $k_1=\beta_1$ and $k_2=1$, Eq. (20) reduces to that for orthotropic elastic materials. It should be noted

that, if the piezoelectric effect vanishes, the case conditions ($k_1^2 - 4k_2$, $k_1^2 - 4k_2 = 0$ and $k_1^2 - 4k_2 > 0$) and all the eigenconditions obtained in this paper can be reduced to those derived by Choi and Horgan (1977) for orthotropic elastic materials.
4. The results of stress decay lengths for some engineering piezoceramic materials are provided. The decay lengths of all the piezoceramics discussed here are larger than that of isotropic materials. Among these materials, PZT-5H has the largest decay length, and it is 24% larger than that of isotropic materials.
5. The results show that the stress decay lengths for piezoceramic materials with an electric field in the x_3-direction are larger than those with zero electric field, and the decay length of PZT-5H with electric field is 11% larger than that with zero electric field.

Acknowledgements

This work was supported by the Office of Naval Research through the MURI program at Rutgers, The State University of New Jersey.

References

Choi, I., Horgan, C.O., 1977. Saint-Venant's principle and end effects in anisotropic elasticity. Journal of Applied Mechanics 44, 424–430 (Transactions of the ASME).

Data Sheet, 1990. Piezoceramics. Vernitron Piezoelectric Division, Bedford, Ohio.

Dogan, A., Newnham, R.E., 1994. Flextensional Cymbal Transducer. USA Patent application, PSU Invention Disclosure No. 94-1375.

Horgan, C.O., 1989. Recent developments concerning Saint-Venant's principle: an update. Applied Mechanics Reviews 42 (11), s101–s111.

Horgan, C.O., 1996. Recent developments concerning Saint-Venant's principle: an update. Applied Mechanics Reviews 49 (10), 295–303.

Miller, K.L., Horgan, C.O., 1995. Saint-Venant end effects for plane deformations of elastic composites. Mechanics of Composite Materials and Structures 2, 203–214.

Newnham, R.E., 1997. Molecular mechanisms in smart materials. MRS Bulletin 22, 20–34.

Newnham, R.E., Xu, Q.C. and Yoshikawa, S., 1992, Transformed Stress Direction–Acoustic Transducer. U.S. Patent 4,999,819.

Park, S.B., Sun, C.T., 1995. Effect of electric field on fracture of piezoelectric ceramics. International Journal of Fracture 70, 203–216.

Rogacheva, N.N., 1994. The Theory of Piezoelectric Shells and Plates. CRC Press, Inc, Boca Raton, Florida.

Ruan, X., Danforth, S.C., Safari, A., Chou, T.-W., 1999. A theoretical study of the coupling effects in piezoelectric ceramics. International Journal of Solids and Structures 36, 465–487.

Tiersten, H.F., 1969. Linear Piezoelectric Plate Vibrations. Plenum Press, New York.

Visual Numerics, Inc., 1994. IMSL Math/Libary, Houston, Texas.

Zelenka, J., 1986. Piezoelectric Resonators and Their Application. Elsevier, Amsterdam, Netherlands.

Zhang, Q.M., Chen, J., Wang, H., Zhan, J., Cross, L.E., Trottier, M.C., 1995. A new transverse piezoelectric mode 2–2 piezocomposite for underwater transducer applications. IEEE Trans. Ultrason. Ferroelect. Frequ. Cont. 42 (4), 774–780.